

Guided wave-based rail flaw detection technologies: state-of-the-art review

Hao Ge¹, David Chua Kim Huat², Chan Ghee Koh²,
Gonglian Dai³ and Yang Yu⁴

Abstract

The unavoidable increase in train speed and load, as well as the aging of railway facilities, is requiring more and more attention to rail defects detection. As a promising tool for rail, in-service high-speed inspection, guided wave-based detection technologies have been developed in succession by researches in the past two decades. However, there is a lack of a systematic review on the developments and performances of these technologies. This article reviews ultrasonic rail inspection methods comprehensively with the focus on the state-of-the-art technologies based on guided wave. Different excitation options, including train wheel, electromagnetic acoustic transducer, pulsed laser, air-coupled, and contact piezoelectric transducer, are described, respectively, along with their inspection sensitivities, regions, and potential speeds. Finally, future challenges and prospects are discussed to a certain extent to provide references for researchers in this area.

Keywords

Rail inspection, rail defects, guided wave, non-destructive testing, non-contact detection

Introduction

Rails are constantly subjected to rolling contact pressure, bending forces, thermal and residual stresses in its service.¹ The increase in axle loads, train speed, traffic frequency, and so on, causes ever-increasing contact forces, which may damage the rails. Rail damage mainly includes rolling contact fatigue (RCF) and internal defects.^{2,3}

As the most common rail damage detection technology, ultrasonic bulk wave-based inspection technique has been used to detect rail defects since the 1960s.⁴ Currently, this technology is based on the fluid-filled wheel probe inside which piezoelectric transducers are placed in several directions.^{5,6} They generate and detect the ultrasound wave in the pulse-echo manner with liquid couplant which is necessary between the transducer and rail.⁷ However, several shortcomings still exist in this technology, such as low speed (typically less than 25 km/h), high attenuation, difficulties in detecting the vertical split defects, and a requirement of coupling agent.^{7–10} The main drawback of the wheel-based ultrasonic detection systems is that surface defects will reflect the ultrasonic wave and hinder its incidence, so that the serious internal defects may be missed.^{3,7,8} Moreover, the frequency adopted in the traditional ultrasonic wave detecting technology is high, resulting in large energy

attenuation and low detection rate for defects in the aluminothermic welds.^{8,9,11} As a result, derailments caused by crack still frequently occur around the world. In the United Kingdom in 2000, a derailment caused by deep transverse crack in the rail head led to Hatfield railway accident, in which 4 passengers were dead while 70 people were seriously injured.^{12,13} Other major derailments, such as in Superior, WI, in 1992 and Oneida, NY, in 2007, resulting in leakage of hazardous material and evacuation of about 40,000 people.¹³

Researchers are therefore constantly exploring new rail non-destructive testing (NDT) technology and that based on ultrasonic guided wave is emerging, which has

¹Changjiang Institute of Survey, Planning, Design and Research, Wuhan, China

²Department of Civil and Environmental Engineering, National University of Singapore, Singapore

³School of Civil Engineering, Central South University, Changsha, China

⁴School of Civil and Environmental Engineering, Faculty of Engineering and Information Technology, University of Technology Sydney, Ultimo, NSW, Australia

Corresponding author:

Yang Yu, School of Civil and Environmental Engineering, Faculty of Engineering and Information Technology, University of Technology Sydney, Ultimo, NSW 2007, Australia.

Email: yang.yu@uts.edu.au

greatly improved the efficiency and speed of rail damage detection.^{3,8,14}

To date, the application of guided waves in NDT has been studied for more than 40 years. Worlton¹⁵ was the first researcher to realize the possibility of damage detection based on guided wave. The textbook wrote by Rose¹⁶ in 1999 introduced the theory and NDT examples of guided wave. Different from ultrasonic bulk wave, guided wave has the ability to travel long distances with low attenuation and to cover the whole cross section of the waveguide.^{17–19} As the stress waves propagate in the elongated structure, reflections, refractions, and mode conversions will be continuously formed by the interaction between stress waves and structure boundaries, resulting in the generation of complex wave packets propagating forward, which can be called as guided waves.²⁰

Ultrasonic guided wave detecting technology can realize rapid excitation from a single transducer, long-range inspection of elongated structure, such as pipe,^{21–24} rod,²⁵ plate,^{26–28} and rail.

It was first applied in pipe and plate damage detection as their dispersion equations are easy to solve. Subsequent studies and experiments proved that guided wave performs well for the damage detection of elongated structures with the symmetric cross section.^{29–31}

With the development of semi-analytical finite element (SAFE) method and calculation ability of computer, the possibility of applying guided wave in rail damage detection has been constantly explored in the past two decades, which shows that rail guided wave-based detection has many advantages over the bulk wave-based detection. Guided wave propagating along the rail is sensitive to rail vertical defects and they are not significantly attenuated by weld material, enabling aluminothermic welds to be tested.^{8,11,32}

Rail NDT technologies based on guided wave have become more and more promising, though many of them are still in the theoretical and laboratory research stage. Research articles about guided wave-based rail flaw detection have been published constantly;^{12–14,20,32–41} a thorough literature review is highly necessary to present the current research situation, existing technologies, and development tendency. Therefore, this article was completed to summarize the developed rail detecting technologies based on guided wave, and their advantages and application conditions are described. It also gives a good understanding of the challenges that the existing technologies have in ensuring the detection reliability and practicability. Moreover, the development trend in the future is prospected.

The article comprises five sections. Section “Types of defects in rail” introduces various rail defects from different perspectives of classification. The dangerous

level of different rail damages is also presented. In section “Dispersive characteristics of guided waves in rail,” the theory of rail guided wave is explained, followed by the description of dispersion and multimode phenomenon. Section “Short-range rail NDT technologies” reviews existing guided wave-based rail NDT technologies together with discussion and comparison of their disadvantages in practical applications. The last section presents the conclusions and some key factors for the technology development in the future.

Types of defects in rail

The rail service defects are primarily determined by the manufacturing quality, daily maintenance, and the loading from the trains.³ Vehicle load is the main source of rail bending and shear stresses while the rail is also subjected to thermal stress, residual stresses, and corrosion.^{42–45}

Defect classification based on location

Rail defects can be classified as rail head defects, web defects, and foot defects based on the damage location. Rail head defects can be further divided into surface and internal defects: the former includes shelling, flaking, burned head, head checking, spalling, crushed head, and rail wear, while the latter refers to head transverse fissures, engine burn fractures, horizontal split defects, and vertical split defects.^{46–53} The surface defects of rail head are easy to be detected while the internal ones might remain hidden until they reach the surface. The report released by the Federal Railroad Administration (FRA) Office of Railroad Safety⁵⁴ has illustrated different types of rail defects in detail.

The web defects represent any progressive damage occurring in the rail web, including web separation defects, split web defects, piped defects, and bolt hole cracks. Rail web defects are mainly caused by residual stress from welding or non-metallic inclusions.^{55,56}

Although the majority of rail defects are generated on the rail head, there are still a significant number of defects found on the rail foot. Rail foot damage should be paid more attention as it is easy to occur and may lead to sudden rail fracture. Most importantly, they cannot be detected by the commercial ultrasound detection vehicle. This type of rail defect mainly includes vertical (longitudinal) crack in foot, broken base, and base nick.^{3,54,57}

Defect classification based on origin

The second way of classifying rail defect is based on its origin.³ Three types of defects can be specifically classified based on this method: defects caused by improper

handling, rail manufacturing defects, and the rail wear because of long service. Improper handling of rails is mostly due to wheel spinning or sudden train brake, which will cause the defects, such as the engine burn and welded burn fracture.^{57–59}

Rail manufacturing defects are originally caused by the inclusions of non-metallic origin and mechanical drilling; as a result, local stress concentration is generated under the continuous vehicle load, which finally leads to the origination of the flaws, such as the weld defect, vertical, or horizontal split defect and bolt hole crack.^{60,61}

The last type of defect includes shelling, spalling, and wear that are caused by abrasive wear of the RCF, which mainly occurs in the surface and subsurface of rail head.^{1,62,63}

Defects classification based on direction

Two types of defect can be classified based on the direction of flaw development, including transverse (extending in the rail transverse plane) and longitudinal defect (extending in the longitudinal (vertical or horizontal) plane).^{54,64} Transverse fissure, detail fracture, and engine burn fractures are typical transverse defects, which primarily grow in a plane perpendicular to the rail extending direction. On the contrary, vertical split defect, horizontal split defect, and broken base can be regarded as longitudinal defects.

However, not all rail defects are dangerous. A critical defect is one that may lead to derailment and affect the safety of running train. Non-critical defect occurs in the rail but does not affect its structural integrity or the safety of the train.⁶⁵

According to the report of railway accidents that took place in the United States between 2005 and 2014, which was released by the FRA Office, transverse fissure caused the most railway accidents and was responsible for 21.7% of the total 2653 accidents, resulting in about US\$113 million economic loss.^{54,66} Accidents caused by head check and shelling occupy a proportion of 17.3%. Accidents caused by various rail damages are illustrated by proportion in Figure 1.

Rail break may happen from a number of causes, including rail foot corrosion, bolt hole, weld failure, internal defect, and so on. Figure 2 shows the rail breaks across all Network Rail (UK) routes during the periods of 2010–2011 and 2013–2014.^{55,67,68}

In total, 171 rail breaks were recorded on Network Rail infrastructure between 2010 and 2011, out of which 67 cases were due to rail foot defects (about 39%). From 2014 to 2015, 54 out of 98 rail breaks were caused by rail foot defects (about 55%). It can be seen that the proportion of rail break caused by rail foot damage increases by 16%, though the total number of

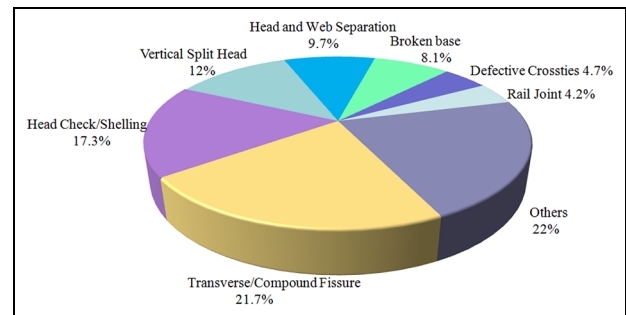


Figure 1. Accidents caused by different rail damages between 2005 and 2014 in the United States.

rail break accident declines. That is probably owing to the fact that rail bottom cannot be successfully detected as it is the blind area for the current detecting technology based on ultrasonic bulk wave. By comparing the data in Figures 1 and 2, it can be concluded that while most derailments are caused by rail head damage, rail foot defect is more likely to cause rail break.⁶⁹ The inspection of rail foot defect is highly essential in the future.

Dispersive characteristics of guided waves in rail

Theory of SAFE method

The application of guided wave in rail is usually quite challenging because of the dispersive nature and existence of multiple modes, which would reduce the resolution of the testing system.^{8,70,71} To select ideal guided wave modes and optimize excitation parameters, the dispersion characteristic of waveguide would be analyzed first.

The dispersion analytical solution of the waveguide with simple cross section, such as cylinder, ellipse, and rectangle, was obtained previously while that is not possible for waveguides with complex cross sections.^{72–74} To analyze the propagation characteristics of rail-guided wave, numerical methods, including the finite element method (FEM)^{12,75–77} and boundary element method (BEM),^{78,79} were respectively adopted. However, these traditional numerical methods are tedious and unable to simulate the wave propagation in infinite waveguide. They also have difficulty in classifying and tracking modes at higher frequencies. SAFE method was demonstrated by Aalami⁸⁰ in 1973, which provides an ideal tool for dispersion analysis of waveguides with arbitrary cross section including the rail.

For this method, only a bi-dimensional element discretization of the cross section is needed. Instead of the conventional finite element interpolation functions

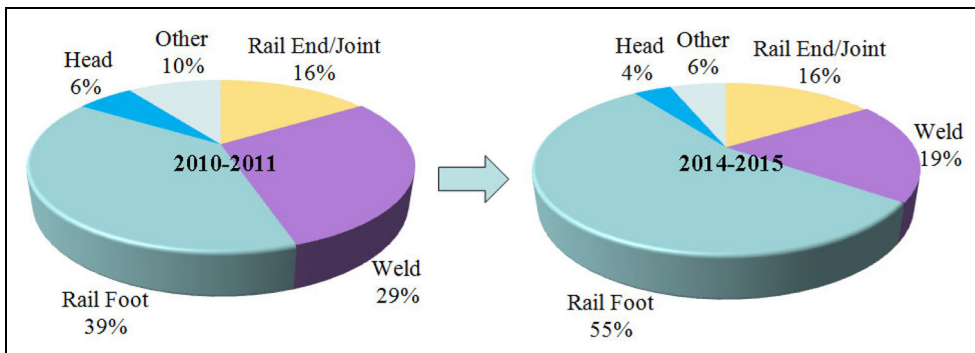


Figure 2. Distribution of rail breaks by types in Network Rail (UK) routes.

adopted by the FEM, complex exponential functions are adopted to describe the waveguide displacements in the wave propagation direction, which have the advantages of avoiding the polynomial approximation of the displacement field and predicting waves with very short wavelength.^{41,81} Meanwhile, they can reduce the time consumption significantly compared to the three-dimensional (3D) FE model.

It has been widely used to obtain the propagative solutions to guided waves in pipe, laminated composite plate, and other waveguides with arbitrary cross section.^{41,82-87} Gavrić⁷⁷ first adopted the SAFE method to calculate dispersion curves and mode shapes for rails.

Pantano and Cerniglia³⁶ and Wilcox et al.⁸⁸ developed a standard software for rail dispersion analysis based on this method. Similar works have been conducted for analysis and selection of rail-guided wave modes in previous works.^{8,12,32,41,89,90} Then, Bartoli et al.⁹¹ extended the SAFE method to consider the rail damping by incorporating complex stiffness matrices; both the hysteretic viscoelastic model and Kelvin–Voigt viscoelastic model were analyzed to make a comparison, and the frequency-dependent attenuation and energy velocity were calculated. Furthermore, rail supports were considered in the SAFE model by Nilsson et al.⁹² and Ryue et al.^{93,94} Nilsson et al. developed one layer of support representing rail pad meshed by finite elements, while Ryue et al. adopted a layer of equivalent springs to simulate the rail supports. Li et al.⁹⁵ have calculated the rail dispersion considering multiple layers of supports consisting of pads, sleepers, and ballast by measuring the pad and ballast stiffness based on field test. The results showed that rail support has significant influence on the rail dispersion and dynamic response but the effect is limited to below 1 kHz.^{75,95,96}

Guided wave can also be used to measure rail axial force. Damljanović and Weaver⁹⁷ investigated the stress in rail based on the wavenumber measured by a scanning laser vibrometer, and considerable length of rail without sleepers was adopted in the experiment.

Chen and Wilcox⁹⁸ analyzed the influence of the axial force on rail guided wave propagation by the FEM, which is a tedious method difficult to be adopted at higher frequencies. Recently, the SAFE method was extended by Loveday⁹⁹ to consider axial force by introducing additional term in the strain energy, which was demonstrated trivial and efficient to investigate the effect of axial force on evanescent waves. In summary, the SAFE has been proved to be able to analyze not only the dispersion of unconstrained rail but also that with supports, damping, and axial force.

Software

Several commercial software, such as Disperse, Rail Dispersion, and GUIGUW, have been developed for the solution of dispersion curve of waveguide. Disperse was created by Lowe and Pavlakovic and was licensed by Imperial College Consultants.¹⁰⁰ It is an interactive window program that can calculate the dispersion curves for plate and cylindrical structures with elastic or viscoelastic material. However, this program is not good enough for calculating the dispersion curve of rail which has a complex section shape.

Rail Dispersion is a specially developed software for calculations of rail dispersion curves and wave structures, as shown in Figure 3.¹⁰¹ Cross sections of various shapes can be drawn by the CAD and input in the Rail Dispersion as a DXF file. Then, GiD software can be adopted to generate the cross-section mesh. Material and frequency parameters can be set conveniently in the window before each calculation. Both the isotropic and anisotropic materials can be considered in this software.^{101,102} Besides the illustration of the dispersion curve, Rail Dispersion has many other functions, such as showing wave structure of a selected mode and dominant mode display. Dominant mode value (DMV) is defined as the ratio of averaged displacement of selected nodes to the maximum displacement of all nodes in the dominant mode display module. Only the modes with

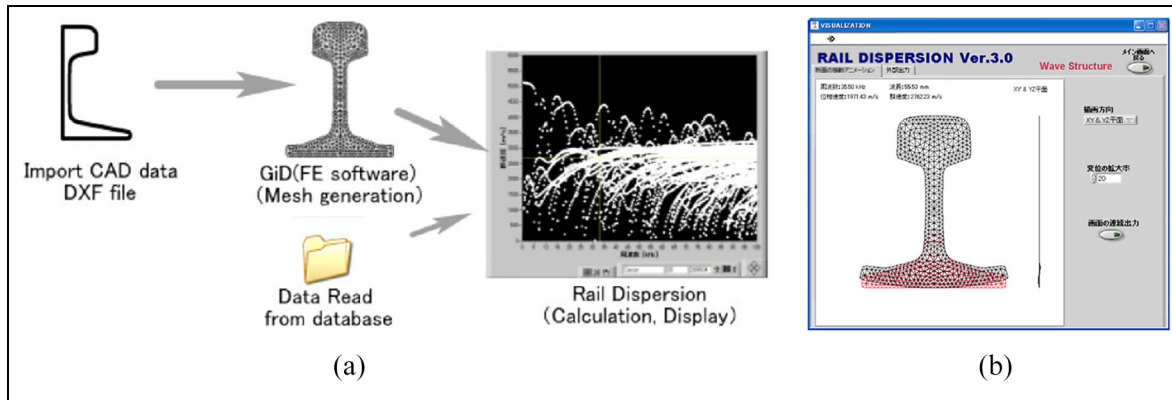


Figure 3. Rail Dispersion software: (a) schematic diagram of operation steps and (b) graphical user interface.¹⁰¹

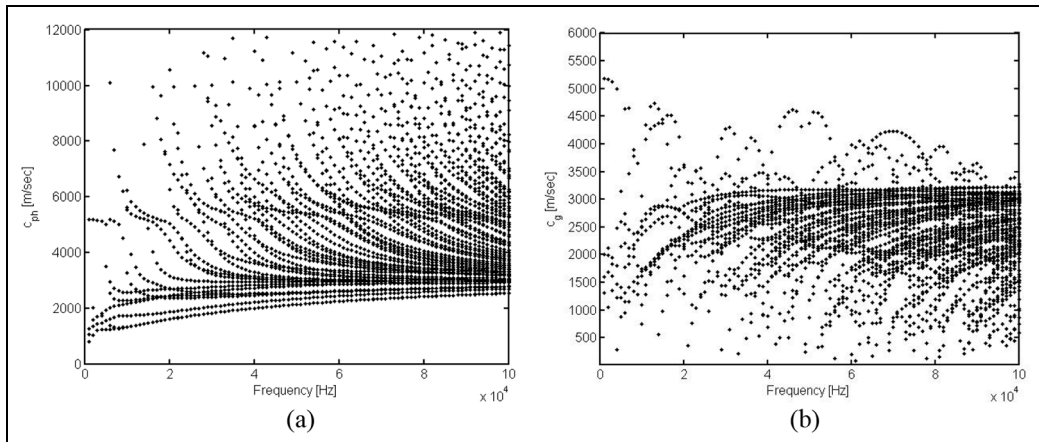


Figure 4. Dispersion curves for UIC 60 rail: (a) phase velocity dispersion curve and (b) group velocity dispersion curve.

DMVs larger than pre-set threshold can be displayed in the dispersion curves, making it convenient for the users to select the ideal mode.

Another software that was developed for dispersion calculation is GUIGUW, which was written in MATLAB code. This software was designed to establish SAFE formulations in the user-friendly graphical interface.¹⁰³

Users can select one of the three options in main window, including cylindrical waveguides, platelike waveguides, and generic cross-section waveguides, to define the section shape. The waveguide with arbitrary cross-section shape can be built in the last module through establishing the coordinates of the cross-section perimeter; the coordinates can be directly inputted as a .txt file. The second panel Guide can be accessed for material properties definition through setting density, Young's modulus, and Poisson's ratio visually. Then, the frequency range and calculation step number can be set in the Solver panel.

After the computations, the Output panel can display different properties of dispersive curves, such as wave number, phase velocity, group velocity (for undamped waveguides), and attenuation (for damped waveguides). It can also display the wave structures of different points in the dispersive curve, which can be utilized to select the ideal mode for detection. Detailed instructions for GUIGUW have been introduced in Bocchini et al.¹⁰³

The phase velocity and group velocity dispersion curves for a UIC 60 rail section using the software are shown in Figure 4. The frequency range selected for analysis is between 0 and 100 kHz with interval of 1 kHz. The elastic modulus, density, and Poisson's ratio are 206 GPa, 7850 kg/m³, and 0.3, respectively.

Short-range rail NDT technologies

In addition to the rail detection technologies based on guided wave, other rail NDT technologies have also

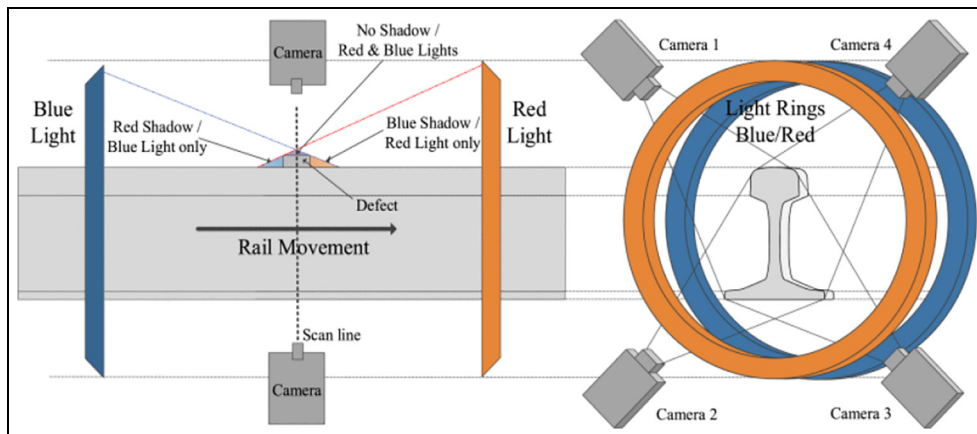


Figure 5. One configuration scheme of visual detection technology.¹⁰⁴

been developed to detect the rail defects, such as computer vision-based inspection technology, vibration-based detection technology, electromagnetic-based detection technologies, and acoustic emission inspection technology. However, they can only detect the rail defects in local area with a low detection efficiency.

The basic principle of visual detection technology is to take the image of rail surface with the CCD camera, as shown in Figure 5,¹⁰⁴ and subsequently obtain the information of the rail damage based on the image processing techniques, such as the convolutional neural network and other deep learning methods.^{104–107}

Several vehicles based on this technology have been reported in previous works.^{108–110} The image-based automatic detection method has the advantages of non-contact and fast detection speed, but it can only detect the rail surface defects, and the detection accuracy and reliability need to be further improved.

For the vibration-based detection method, one technology is developed to realize online monitoring of rail irregularity by monitoring the acceleration of the train,^{111–117} as shown in Figure 6. However, at present, this detection method can only detect irregularities, such as insulated joints, shelling, head checking, spalling, and rail wear.^{112–117}

Electromagnetic-based detection technologies, such as eddy current, magnetic flux leakage (MFL), and alternating current field measurement technology (ACFM), can detect defects near the rail surface by introducing current or electromagnetic field into the rail and detecting the corresponding electromagnetic response.¹¹⁸ Due to skin effect, deep defects located at rail web and foot cannot be well detected by electromagnetic detection technology, and the distance between the detection coil and rail surface should be less than a few millimeters; otherwise, the detection sensitivity will be significantly reduced.



Figure 6. Axle box acceleration system used with close-ups of the GPS antenna and an accelerometer.¹¹⁶

The essence of eddy current detection is to identify the change of coil impedance.¹¹⁸ This technology is sensitive to lift-off distances (no more than 2 mm away) and is only valid for surface defects detection.¹¹⁹ A typical speed of 75 km/h has been achieved in the developed vehicle as shown in Figure 7.^{120–124}

The MFL detection technology is a very important NDT method which has been widely used for detecting defects in ferromagnetic structures.^{125–127} MFL detection technology is good at detecting surface or near-surface transverse defects, while deep internal cracks cannot be detected by this technology. A hi-rail vehicle based on MFL detection technology has been produced by the FRA as shown in Figure 8. The maximum inspection speed achieved is about 35 km/h in the field tests.^{117,128}

ACFM technology is suitable for rail RCF detection and capable of detecting at high speeds.^{129–134} First, this technology introduces a uniform current to the surface of the measured specimen. When there are surface



Figure 7. Rail detection vehicle based on the eddy current.¹¹⁷

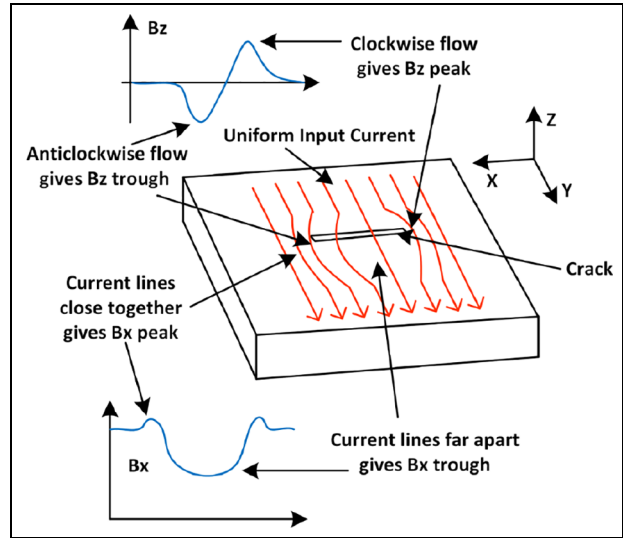


Figure 9. Principle and field directions of ACFM.¹²⁹



Figure 8. Hi-rail inspection vehicle based on MFL.¹⁷

defects in the tested structure, the current line will be cut off, forcing the current to flow below the defect and around the defect end. The defect can be detected by measuring the magnetic field (Figure 9). Relevant detection equipment has been developed since 2000, among which the maximum detection speed can reach 3 km/h with rail cracks as small as 2 mm detected.^{117,135}

The AE-based detection technique identifies defects based on the ultrasonic waves released by crack initiation and propagation. In view of its successful applications in structural health monitoring,^{136,137} the potential has been explored to apply it in rail damage detection.^{138,139}

It has the advantages of in-service monitoring and unnecessary artificial excitation. However, wheel-rail contact rolling noise often leads to low signal-to-noise ratio (SNR) of AE signal; various advanced denoising algorithms have been developed to increase the SNR of rail AE signal, proving that it is possible to extract rail damage information in the field environment.^{140–144}

Furthermore, it is still a challenge to make a quantitative assessment of rail defect based on the AE technology, highlighting the need for more research in this area.¹⁴⁵

Long-range rail NDT technologies based on guided wave

With the development of rail guided wave detection technology, various detection devices have been designed and manufactured to make the detection of rail defects in field.

Artificial hammer excitation

With this method, guided wave is excited by the hammer or impactor.¹⁴⁶ It is based on pitch-catch mode with the mounted accelerometers, contact piezoelectric sensors, non-contact air-coupled, or electromagnetic acoustic transducers (EMATs) installed as receivers. Rose et al.⁸ conducted several field experiments showing the ideal excitation frequencies, frequency-related wave attenuation, and rail dispersive curve based on this technology. It is easy to operate but not applicable to on-board automatic detection.

Guillermo et al.¹⁴⁷ have developed detection equipment based on this technology, which is composed of National Instruments data acquisition module, PCB impact hammer, PCB triaxial accelerometer, and LabView software, as shown in Figure 10. The hammer impact was applied at four specified points, and the signals were measured in two directions (X and Z). Post-processing was subsequently carried out to obtain the

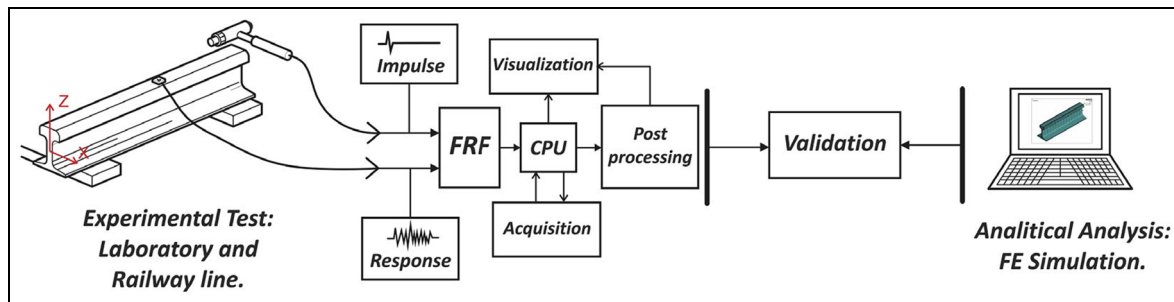


Figure 10. Experimental test based on impact hammer excitation.¹⁴⁷

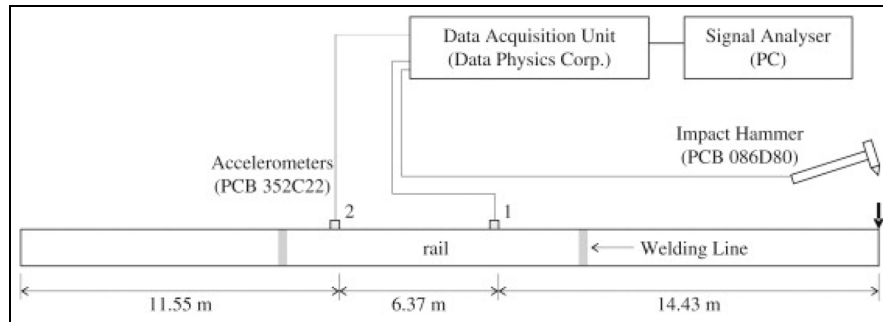


Figure 11. Experimental scheme with impact hammer as an exciter.⁴⁰

frequency response function (FRF) graph based on the Fourier transform.

Ryue et al.⁴⁰ performed the experiments as shown in Figure 11 to validate the rail dispersion properties with a miniature impact hammer to generate the broadband signal. The excitation frequency range was limited to 40 kHz. Accelerometers were set along the rail at different positions; the signals received by them were processed using the short-time Fourier transform for time-frequency analysis to identify.

Contact transducers excitation

Institute of Maritime Technology. The way to excite guided wave based on the contact transducers is reliable and effective. An early system named Ultrasonic Broken Rail Detector (UBRD) has been developed by the Institute of Maritime Technology (IMT)^{34,148,149} to detect rail breaks in heavy haul railway; contact piezoelectric transmitters and receivers were installed along the rail in pitch-catch mode and the typical distance between them is up to 1 km (Figure 12). Ultrasonic signals were transmitted every few minutes, and the alarm was triggered when the signals were not received by the receivers. However, it is difficult for this system to detect the minor damages in rail.

It was reported that three breaks were detected in 15 months on a 34-km long railway line and some internal defects.¹⁴⁹

The Welding Institute. The prototype of the Welding Institute (TWI) was developed in the MONITORAIL project, funded by the European Union, and it was in the stage of laboratory test only.^{150–153} The system employed the piezoelectric elements (PZT) that were permanently bonded onto the rail surface (head, web, and foot), as shown in Figure 13. The locations where PZTs were attached to the rail cross section were chosen carefully, so that specific wave modes that uniquely occur in each section (head, web, and foot) can be generated. The detection was based on the pulse-echo response of each wave mode in different sections of the rail.

In their laboratory test, a 10-cycle tone burst signal with a center frequency of 70 kHz was used to excite the desirable wave modes on the rail foot and transverse slots were cut on one side of the rail foot to simulate defects. The results showed that a crack with 5 mm in depth is detectable at a distance of 4 m (from sensor to defect).¹⁵⁰ Commercial guided wave ultrasonic system, Teletest, was used as an arbitrary function generator to excite the PZT and to collect the responses from the rail. A combination of features, such as the first-order statistics from time domain, power spectral density (PSD) measures, and wavelet features, was extracted to perform damage classification based on the support vector machine (SVM).^{151,153}

One of their test results showed that if the rail fastening systems are well insulated from the rail,



Figure 12. Fixed transducer and power supply.³⁴

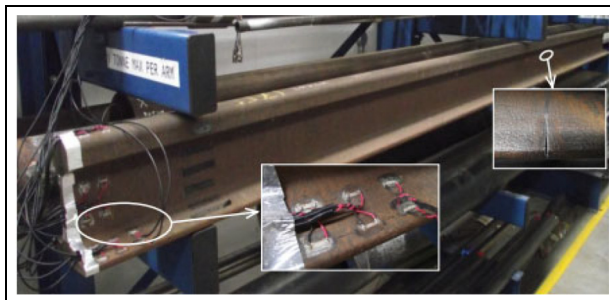


Figure 13. The mounted piezoelectric transducers at the end of rail.¹⁵³

however, the effect of fastening system on wave reflection can be alleviated.^{151,152} It is also evident in the experiments that even in the case of large defects, changes in the environmental conditions (temperature and humidity) increase the challenge for the interpretation of the acquired signals.¹⁵³

Imperial College London (G-Scan system). G-Scan used the transducer array all around the perimeter of the rail

(excluding the underside) to generate guided waves in rails, as shown in Figure 14. In total, the G-Scan system used 42 transducers, where 18 were mounted on the head, 12 mounted on the web, and a further 12 on the foot, which were dry-coupled to the rail using a combined mechanical and pneumatic control system. It worked in pulse-echo mode and was able to detect the vertical and thermite weld defects. It was claimed that the transducers were driven with an appropriate-weighted signal to impose the desired wave mode.^{14,154,155}

The system used reflection coefficient spectra as a means of detecting rail features. The prototype has been tested on a number of rail samples containing a variety of artificially introduced defects. Good agreement was obtained between the predicted and measured reflection coefficient maps.¹⁵⁵

Nagoya Institute of Technology. Rail guided wave experiment based on the excitation of contact angle beam transducers was conducted in Nagoya Institute of Technology, Japan. The experiment showed that the vertically vibrating mode was attenuated by fastening systems, while horizontally vibrating mode had a better performance in detecting rail foot defect. The experimental configuration is shown in Figure 15,^{101,156} and the rail damage was identified based on the amplitude of the reflected wave.

Furthermore, the Rayleigh-like wave with a velocity of about 3000 m/s at 100 kHz was excited in their research. The optimal incident angle of the wedge was determined as 55° based on Snell's law. Test results showed that a 20-mm saw notch located at a bottom edge 10.5 m away from the exciting transducer was identifiable, though 20 fastenings existed between the transducer and the defect.

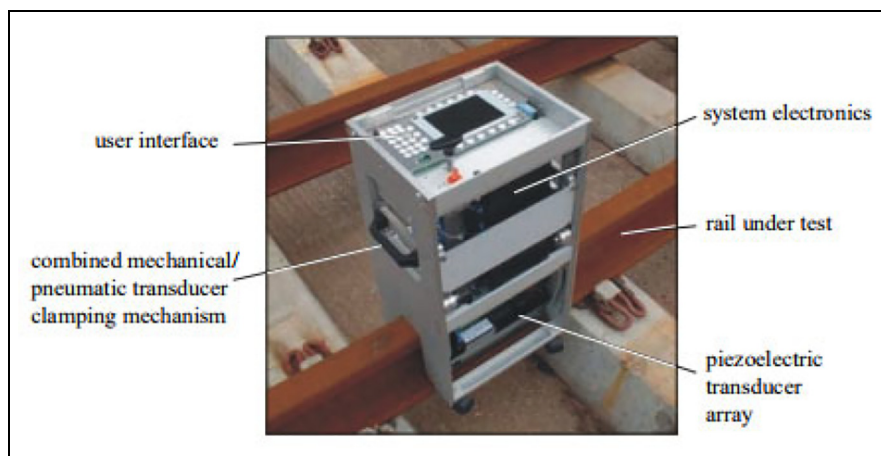


Figure 14. G-Scan system developed by Imperial College London.¹⁵⁴

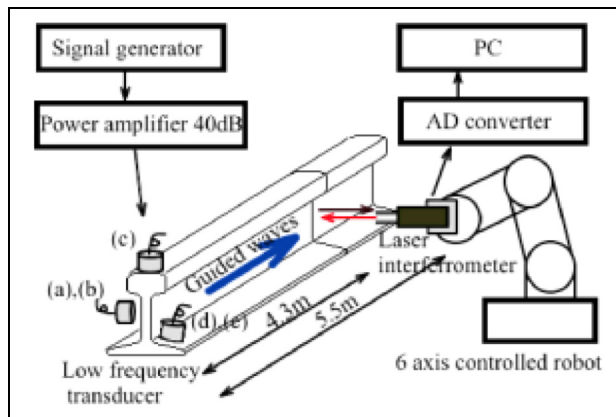


Figure 15. Experimental scheme with the contact transducers to excite guided waves.¹⁰¹

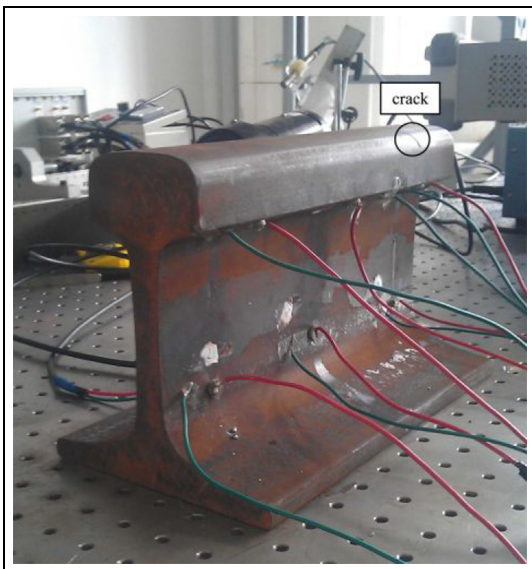


Figure 16. Contact piezoelectric wafers in the laboratory experiment.¹⁵⁷

Guangzhou University. A new 3D diagnostic imaging technique based on contact excited guided wave was developed, which was able to quantitatively visualize the rail defects.¹⁵⁷ As shown in Figure 16, nine circular piezoelectric wafers (diameter: 10 mm, thickness: 1 mm) were subsequently mounted on the rail surface to form the wave sensing paths (Figure 17). A three-cycle Hanning window-modulated sinusoidal pulse with a central frequency of 200 kHz was used as the input signal. It was then amplified by a linear power amplifier (PiezoSys® EPA-104) and output by an oscilloscope (SDS1204CFL).

The principle of this method is shown in Figure 17, based on which a set of equations can be established as follows

$$\left\{ \begin{array}{l} \left(\frac{L_{A_i-D}}{V} + \frac{L_{D-S_j}}{V} \right) - \frac{L_{A_i-S_j}}{V} = \Delta t_{i-j} (i, j = 1, 2, \dots, N, \text{ and } i \neq j) \\ L_{A_i-D} = \sqrt{x_D^2 + y_D^2 + z_D^2} \\ L_{D-S_j} = \sqrt{(x_D - x_j)^2 + (y_D - y_j)^2 + (z_D - z_j)^2} \\ L_{A_i-S_j} = \sqrt{x_j^2 + y_j^2 + z_j^2} \end{array} \right. \quad (1)$$

A series of spatial curves can be plotted based on equation (1). The inspected rail can be meshed using $K \times L \times M$ nodes. The smaller the distance from the node to the spatial curves, the higher the probability that defect exists at this node, and the mesh nodes located on the spatial curve have the highest probability. A cumulative distribution function (CDF), $F(C_{ij})$, is defined as

$$F(C_{ij}) = \int_{-\infty}^{C_{ij}} f(c) \cdot dc \quad (2)$$

where $f(c) = (1/(\sigma_{ij}\sqrt{2\pi})) \exp[-c^2/2\sigma_{ij}^2]$ represents the probability density of damage presence at mesh node (x_k, y_l, z_m) , ($k = 1, 2, \dots, K$; $l = 1, 2, \dots, L$; $m = 1, 2, \dots, M$).

Defining $c_{ij} = ||\chi_i - \mu_{ij}||$, where χ_i is the position vector of node (x_k, y_l, z_m) , and μ_{ij} represents the position vector of the point on the spatial curves that has the shortest distance to node (x_k, y_l, z_m) . Then, the probability of damage presence, $I(x_k, y_l, z_m)$, at the node (x_k, y_l, z_m) can be expressed as

$$I(x_k, y_l, z_m) = 1 - [F(C_{ij}) - F(-c_{ij})] \quad (3)$$

Based on equation (3), field value of each node can be calculated to visualize the probability of rail defects presence. This method has the advantage of locating the possible position of the defects and quantifying them, but it cannot realize the continuous detection.

Laser excitation

Laser excitation technology provides a very attractive solution to guided wave detection of structures. A laser pulse with sufficient power can be adopted to generate stress component in the ablative regime, resulting in elastic waves which propagate through the waveguide.^{158,159} The generated guided wave will be influenced by the flaws and detected by the receiving transducers, such as laser interferometer, contact piezoelectric transducers, and air-coupled transducers.

Compared with the traditional piezoelectric ultrasonic technology, laser ultrasonic technology has the advantages of non-contact, no coupling agent, high energy, and so on. The influence of rail surface

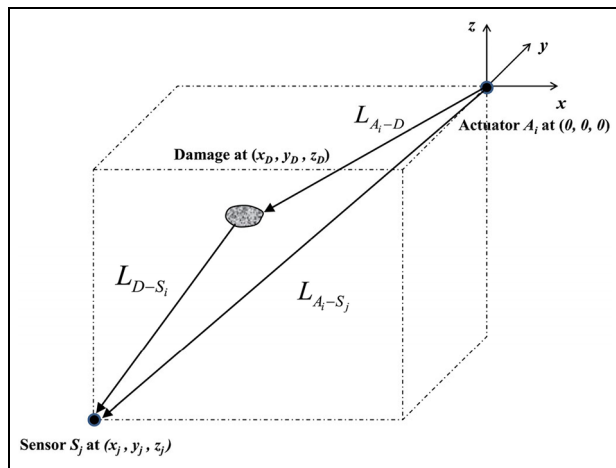


Figure 17. Relative positions among actuator, receiving sensor, and damage in the local coordinate system.¹⁵⁷

roughness and cleanliness on the detection performance of this technology is much less. In addition, laser ultrasonic technology has strong anti-interference ability and can be applied in the harsh environment. When the pulse laser is excited on the solid surface, it can generate the longitudinal wave, transverse wave, and surface wave, detecting both the internal and surface defects of the rail. Meanwhile, it can detect the defects of rail foot which is the blind area for traditional ultrasonic guided wave.^{8,160} To date, different laser-ultrasonic rail inspection systems (LURI) have been developed by several research groups.

Transportation Technology Center Inc.: U-Rail. A LURI (U-Rail) has been developed by Tecnogamma SPA (Italy) and evaluated by Transportation Technology Center Inc. (TTCI). The U-Rail system used high energy laser to generate ultrasonic signals in the rail to monitor the waves propagating along the rail, and it can be installed

in the vehicle and realize rail in-service inspection with higher speed. The system was claimed to be able to dynamically inspect the full rail section, including the rail web and foot,^{161–164} thereby reducing the risk of derailment. An industrial Neodymium: yttrium-aluminum-garnet (Nd:YAG) laser has been specially designed to operate in the harsh railroad environment. It has a power of 50 W and 120 Hz repetition rate. Two air-coupled transducers (with wide-range frequencies from 40 kHz to 2 MHz) were mounted on both sides of the laser transmitter, and the defect identification can be realized by comparing the difference of the two received signals.

The rail flaw inspection system has been installed in a hi-rail vehicle, as shown in Figure 18. In addition to aforementioned inspection unit, a position recording system was used to track the rail and also discern fixtures or other obstacles over the rail. The proposed prototype was tested at the Rail Defect Test Facility (RDTF) located at the TTC, and the tests showed that the rail defects can be successfully detected with a speed up to 32 km/h.^{161–163}

FORCE Technology: automatic LURI. Another track inspection vehicle based on laser ultrasonic technology was developed in Denmark. The integrated detecting system was placed inside the vehicle which was composed of laser exciting systems, power supply units, data acquisition electronics, and signal processing system. The optical subsystem was mounted at the bottom of the car to record its location.^{165–167}

Different from the common methods that used sensors as the receiver, a second laser was installed in the LURI system to detect the rail damage. The laser-excited ultrasonic wave would cause a small surface motion in the nanometer range, leading to a Doppler frequency shift on the scattered light of the receiving laser. Then, the scattered light was coupled into an



Figure 18. Hi-rail vehicle with the laser-based rail flaw inspection system installed.¹⁶²



Figure 19. LURI with optical subsystem.¹⁶⁷

interferometer, and it demodulated the Doppler-shifted light into the variation of light intensity in time domain, based on which, the rail defect was identified.

Several field experiments were carried out at Banedanmark's site near the Storebælt railway tunnel facility in Denmark (Figure 19), proving that it can not only detect the surface, horizontal and vertical flaws in the railhead, but also identify the rail web and foot defects with the speed up to 40 km/h. The battery-operated flaw detector based on the P-scan Lite system was developed to support the automatic LURI system.¹⁶⁷

University of California San Diego: laser-air hybrid ultrasonic technique. University of California San Diego (UCSD) group has been working in the field of non-contact guided wave-based rail inspection system for more than one decade, with the focus on rail head defects detection. The laser-air-coupled hybrid non-contact system was developed with high energy laser to generate guided wave in a slightly ablation regime.^{9,90,168,169} The laser generator was a Q-Switched Big Sky Laser CFR-400 capable of 300 mJ pulse of 10 ns duration on 30 Hz max repetition rate. The frequency range of the air-coupled transducer was very broad, ranging between 40 kHz and 2.25 MHz.^{168,169}

The damage index (D.I.) was proposed to identify the potential defects. When reflection mode was used in the test, the ratio between the features of the echo signal $F_{\text{reflection}}$ and that of the direct signal F_{direct} was expressed as the D.I., as shown in equation (4)

$$D.I. = \frac{F_{\text{reflection}}}{F_{\text{direct}}} \quad (4)$$

In transmission mode, two sensors were installed in one side of the laser source, the D.I. adopted the ratio between extracted features of the signal received by the

further transducer F_{sens2} and that of the closer one F_{sens1} .

The transmission mode had high efficiency in determining the damage severity, while reflection mode was able to locate the defect position.

Various features, including the variance, the root mean square (RMS), and the peak-to-peak amplitude of the threshold wavelet coefficients, were, respectively, used for the D.I. calculation and defect identification.^{170,171} The results demonstrated that the RMS of the wavelet coefficients was the best choice. The prototype has been successfully tested in the field for improvement as shown in Figure 20, and it showed good performance for implementation in rail inspection.^{168,169}

The main drawback of this laser-based system is the presence of the laser, which is quite costly and potentially hard to maintain.⁶⁶ Furthermore, the limited repetition rate of the laser excitation represented a probably insurmountable obstacle toward the increase in the testing speed.^{168,169} One way to resolve these issues is to substitute the laser with a piezoelectric air-coupled focused transmitter, which is able to produce a somewhat similar ultrasound excitation on the rail top surface.

Air-coupled transducer excitation

Another prototype developed by the UCSD group consisting of a cylindrically focused air-coupled piezoelectric transmitter was used to substitute for the laser, as shown in Figure 21.^{13,172–174} The new challenge with this method is the low SNR since most of the energy excited by the air-coupled transmitter is reflected back in air due to the large acoustic impedance mismatch between air and rail.^{66,174} To alleviate reflected signals, a specially focused transmitter has been used in



Figure 20. Laser-air hybrid ultrasonic technique prototype tested in the field.¹⁶⁸

combination with highly resonant impedance matching networks (L-matching networks) in reception. The electrical impedance matching network essentially creates resonant conditions at the frequency of interest at the receivers' side to amplify the signal.^{66,174}

A statistical pattern recognition algorithm based on multivariate outlier analysis was applied to maximize true outliers and minimize false positives.⁶⁶ In this algorithm, n signals received in raw rail were first obtained, and each with m features was extracted. The same type of features was averaged to form the baseline as $\{\bar{x}\}$, and the covariance of the extracted features was calculated as the $[K]$ ($m \times m$ matrix). Then, when $n + 1$ signal is acquired, the deviation of its features (vector $\{x_{n+1}\}$ with a length of m) from the baseline was calculated based on the “Mahalanobis squared distance” as the D.I., as shown in equation (5)

$$D.I._{n+1} = (\{x_{n+1}\} - \{\bar{x}\})^T [K]^{-1} (\{x_{n+1}\} - \{\bar{x}\}) \quad (5)$$

When the calculated D.I. was larger than the proposed threshold value, the defect was confirmed.

Two field tests were conducted at the Rail Defect Test Facility of the TTC in 2014 and 2015, respectively. The results of these tests, evaluated in terms of probability of detection versus probability of false alarms (receiver operating characteristic curves), indicated a good detection performance at speeds of 1.6 and 8 km/h, and much poorer performance at speeds of 16 and 24 km/h.^{66,174}

Train excitation

Theoretical analysis of this approach has been done early by Ryue et al.^{13,93,166–175} Recently, UCSD proposed a new scheme of non-contact receivers, without using active transmitters, as shown in Figure 22.^{176–178} This high-speed ultrasonic rail inspection system was developed based on passively reconstructing the rail's transfer function from the excitations naturally caused by the rolling wheels of a moving train. Multiple pairs of receivers were used to sense the acoustics excited in the rail by the running wheels, and the deconvolution process was used to eliminate the random effect of the excitation and reconstruct a stable acoustic transfer function of the rail.

The basic principle of this method is shown in Figure 23, where the transfer function of the rail between receiver A and B, $G_{AB}(\omega)$, needs to be isolated first, and then the change of $G_{AB}(\omega)$ can be used to identify the defects in the rail.¹⁷⁸ Assuming the wheel excitation spectrum is $W(\omega)$, the frequency response measured at receiver A, $V_A(\omega)$, can be expressed as

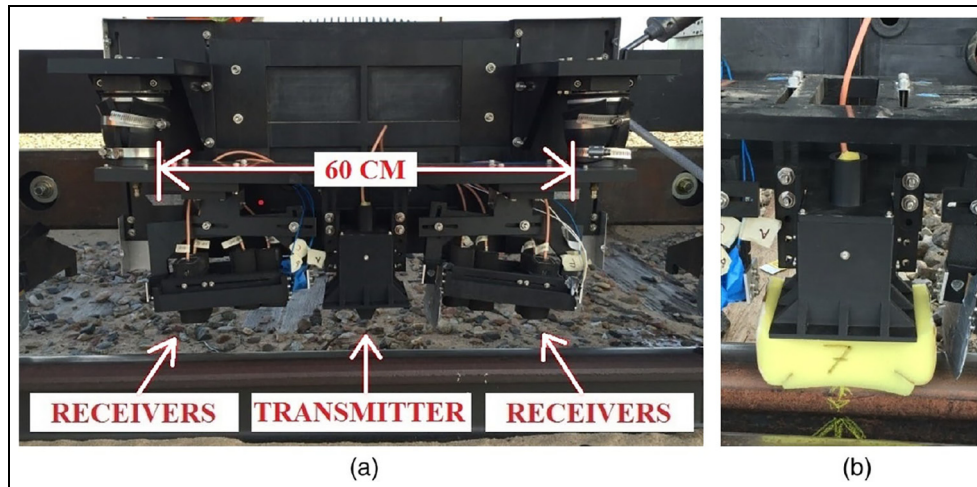


Figure 21. (a) Non-contact air-coupled ultrasonic detecting prototype mounted on a moving cart. (b) Sponge placed between transmitter and rail top surface for testing at sustained speeds.⁶⁶

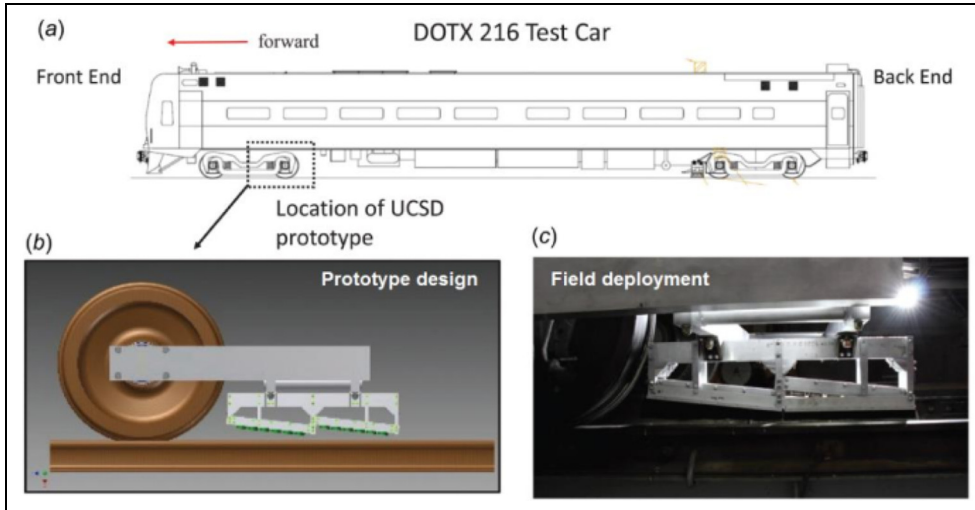


Figure 22. The passive inspection prototype: (a) the FRA DOTX-216 test car and (b) and (c) non-contact air-coupled receivers.¹⁷⁸

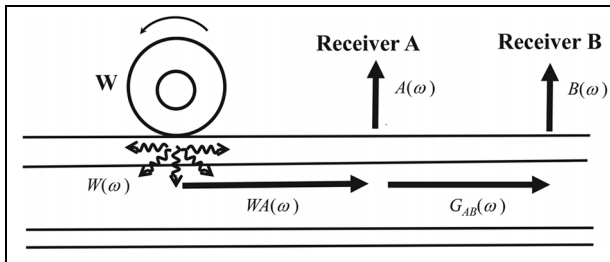


Figure 23. Principle of the detecting method based on transfer function.¹⁷⁸

$$V_A(\omega) = W(\omega) \cdot WA(\omega) \cdot A(\omega) \quad (6)$$

where $WA(\omega)$ represents the transfer function of the rail between the wheel and receiver A , and $A(\omega)$ represents the frequency response of receiver A . Similarly, the response measured at receiver B is expressed as follows

$$V_B(\omega) = W(\omega) \cdot WA(\omega) \cdot G_{AB}(\omega) \cdot B(\omega) \quad (7)$$

The cross-correlation coefficient, $Xcorr_{AB}(\omega)$, between $V_A(\omega)$ and $V_B(\omega)$ can be calculated as

$$\begin{aligned} Xcorr_{AB}(\omega) &= V_A^*(\omega) \cdot V_B(\omega) \\ &= W^*(\omega) \cdot WA^*(\omega) \cdot A^*(\omega) \cdot W(\omega) \cdot WA(\omega) \cdot G_{AB}(\omega) \cdot B(\omega) \\ &= |W(\omega)|^2 \cdot |WA(\omega)|^2 \cdot A^*(\omega) \cdot B(\omega) \cdot G_{AB}(\omega) \end{aligned} \quad (8)$$

where the asterisk * represents complex conjugate, $| \cdot |^2$ means the autocorrelations. As the receiver A and B are of the same type, $A(\omega)$ can be considered equal to $B(\omega)$.

To isolate the $G_{AB}(\omega)$, the autocorrelation of the frequency responses of receiver A or B can be used to divide the cross-correlation, which is expressed as

$$\begin{aligned} NormXcorr_{AB}(\omega) &= \frac{Xcorr_{AB}(\omega)}{Autocorr_A(\omega)} \\ &= \frac{|W(\omega)|^2 \cdot |WA(\omega)|^2 \cdot A^*(\omega) \cdot B(\omega) \cdot G_{AB}(\omega)}{|W(\omega)|^2 \cdot |WA(\omega)|^2 \cdot |A(\omega)|^2} \\ &= \frac{B(\omega)}{A(\omega)} G_{AB}(\omega) \end{aligned} \quad (9)$$

As $B(\omega)/A(\omega)$ is a constant value for the certain receivers, the transfer function is thus isolated. Finally, the time domain signal $G_{AB}(t)$ can be obtained based on the inverse Fourier transform as shown in equation (10), which is used to identify the rail defects

$$G_{AB}(t) = \frac{1}{2\pi} \int_{-\infty}^{\infty} G_{AB}(\omega) e^{i\omega t} d\omega \quad (10)$$

A prototype based on this method has been constructed and tested at the TTC in 2016. Test runs were conducted at speeds with the range from 25 to 80 mph. The results showed the feasibility of a stable reconstruction of the transfer function from the random wheel excitation and the detection of joints and welds in the track.^{177,178} To sum up, the UCSD group has done a lot of excellent work focusing on the rail head defects detection.

An active approach based on train-excited diffused ultrasonic waves (DUW) was developed by Wang et al.¹⁷⁹ In traditional methods, baseline signals will be obtained first to identify the defect-related changes in

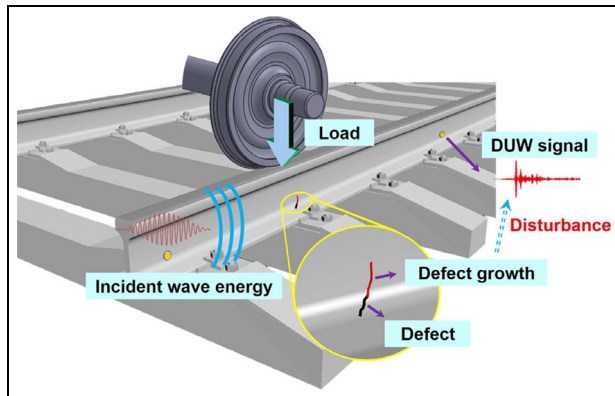


Figure 24. Train-induced defect growth causing disturbance in the received guided waves.¹⁷⁹

the received signals. However, this approach does not need the baseline signals since it detected the rail damages based on the diffuse ultrasonic waves acquired before and after a train passage. As shown in Figure 24, a piezoelectric wafer was installed in the rail web, when the trains passing by, the train induced loads will lead to the growth of defects in the rail, which will thus give rise to the discrepancies between the signals acquired before and after the train's passage.

On this basis, a D.I. R_{cc} , calibrating the decorrelation between the DUW signals acquired before and after a train passage, was proposed in their study to identify the rail defects, the expression of which is shown as follows

$$R_{cc} = 1 - \frac{\int X(t)Y(t)dt}{\sqrt{\int X(t)^2 dt \int Y(t)^2 dt}} \quad (11)$$

where $X(t)$ and $Y(t)$ represent the DUW signals acquired before and after the train's passage, respectively. Consequently, the more severe the defect in the rail, the larger the D.I. (R_{cc}). Field tests were then carried out in Chengdu North Marshalling Station by the researchers, and the defects of switch rails were detected, which demonstrated the reliability of the application of this approach.

The detection method based on train excitation is simple and convenient to operate, it does not need active transmitters as the running train plays the role of it, the high SNR can also be realized. However, it can only detect the damage of a certain section of rail according to the arrangement of sensors and cannot realize continuous detection with the train running.

EMAT excitation

EMATs can be utilized to generate ultrasonic wave in metal structures in a non-contact manner, showing the

promise for in-service defects monitoring. It is generated by a coil inducing a dynamic current in the structure surface, and then a static magnetic field is provided by a permanent magnet. The particles forming the dynamic current circuit will be affected by Lorentz force, and the particles will vibrate under the action of alternating Lorentz force to form ultrasonic wave whose frequency is the same as that of alternating current in the exciting coil.¹⁸⁰

The commercial hi-rail inspection vehicle (Rail-Pro) carrying the EMAT system has been developed by Tektrend with speed up to 15 km/h.^{181,182} However, this technique cannot detect surface defects less than 2 mm deep and has a low ultrasound conversion efficiency.

Dixon and co-researchers adopted EMAT to excite Rayleigh-like surface wave in rails at a frequency of range from 150 to 500 kHz, focusing on the detection of rail head defects.^{183–186} While Wang et al.¹⁸⁷ utilized EMAT-exciting guided wave to identify defects in rail foot, 300 kHz pseudo-Rayleigh waves were excited to detect typical defects in the rail base by the EMATs as shown in Figure 25, which consists of a permanent magnet and meander-line coil. Consequently, the spacing interval between adjacent wires was set to 5 mm to generate 300 kHz pseudo-Rayleigh waves effectively, as the wavelength of 300 kHz pseudo-Rayleigh waves is about 10 mm. The information on the rail defects was deduced from the reflecting signals.

A brief summary of the detecting technologies based on different exciting methods is shown in Table 1, showing the performance and the achievable detecting speeds.

Concluding remarks and challenging issues

Many major derailment accidents in the history were caused by rail damage. With the rapid development of high-speed and heavy haul railway, more and more attention has been paid to the rail damage detection.

Though commercial system, which is based on conventional ultrasonic bulk wave, has been applied to inspect the rail defects for a long time, some disadvantages still exist, such as missed rail bottom detection, surface defects interference, and slow speeds. Reliable technologies that are suitable for the application in moving train are needed to meet the demand for rapid detection of thousands of kilometers of rail. Ultrasonic guided waves have been considered as a promising method to realize high-speed inspection of rail defects with the development of SAFE theory. Such waves, propagating along the rail, are able to cover the whole section of the rail.

The researches of rail NDT technologies based on guided wave have been reported in succession these

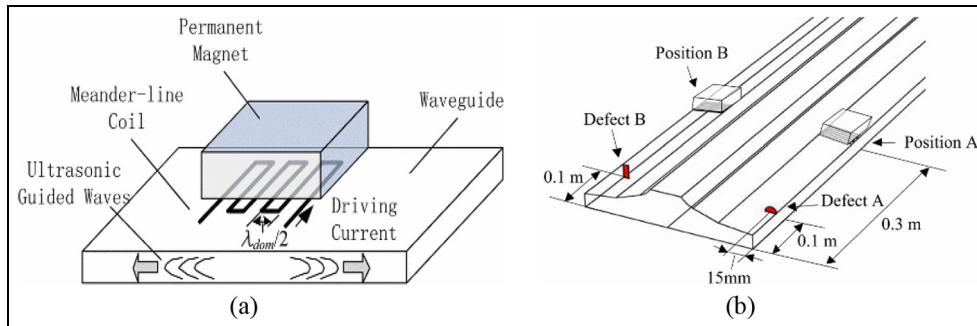


Figure 25. EMAT excitation-based detection: (a) structure of meander-line EMAT with permanent magnet and (b) positions of the EMATs and defects based on pulse-echo mode.¹⁸⁷

Table I. Summary of exciting methods of guided waves in rail.

Exciting method	Performance	Available on-board detection speeds	Limitation of inspection speed
Hammer excitation ^{146,147}	Easy to operate. High SNR. Limited exciting frequency. Cannot realize on-board detection	Unable to realize on-board detection	Unable to realize automatic continuous detection
Contact piezoelectric sensor ^{14,148–157}	Low cost. Coupling agent is required. Cannot realize on-board detection	Unable to realize on-board detection	Unable to realize automatic continuous detection
Laser excitation ^{158–171}	Non-contact and high SNR. Strong anti-interference ability. Suitable for rail foot detection. High cost. Relatively unsafe. Limited repetition rate	40 km/h ¹⁶⁷	Repetition rate
Air-coupled transducer ^{13,66,172–174}	Non-contact. Easy to operate. Low SNR	24 km/h ^{66,174}	Low SNR. Inspection accuracy
Train excitation ^{176–179}	No need for exciting transducer. High detecting speed. Insensitive to small defect	40–120 km/h ¹⁷⁸	Train speed. Inspection accuracy
EMAT excitation ^{180–187}	Non-contact. Insensitive to surface defects less than 2 mm deep. Low ultrasound conversion efficiency	15 km/h ^{181,182}	Pulse repetition frequency
Crack initiation and propagation ^{136–145}	In-service monitoring. Unnecessary artificial excitation. Low SNR	Unable to realize on-board detection	Static inspection technique

SNR: signal-to-noise ratio; EMAT: electromagnetic acoustic transducer.

years. State of the art of the available technologies and prototypes has been comprehensively reviewed in this article.

It also summarized both the limitation and capability of each technology. Based on the review, a number of technical challenges still exist and following prospects can be obtained:

1. The application of guided wave in rail defect detection is still challenging because of the complex cross section of rails. It is definitely necessary to resolve

some problems in rail guided wave detection, such as the ideal modes selection for rail different parts, optimal exciting method for ideal mode, and dispersion reduction.

2. Though rail detection systems based on conventional ultrasonic bulk wave will still remain the main selection in the foreseeable future, non-contact detection methods based on guided wave can potentially detect rail foot defects and provide rail in-service inspection with higher speeds. An integrated commercially available inspection

- system that combining the guided wave-based inspection with other non-contact detection technologies, such as visual inspection eddy currents or ACFM, is promising in the future, which can improve the reliability and avoid the false alarm in rail defects detection. Meanwhile, signal processing system, consisting of signal collection, signal processing, damage analysis, and wireless transmission modules, is required to achieve real-time online monitoring of the rail.
3. During the past 10 years, great efforts have been made to develop the air-coupled sensors for non-contact applications in NDT. Due to the impedance mismatch and loss of signal energy in the air, the inherent disadvantage of low SNR exists in the air-coupled sensors, which makes the system difficult to identify damage information correctly. While it is necessary to develop more robust and sensitive air-coupled sensors, composite SNR enhancement technology combining amplifier with band-pass filters is also recommended to be employed.
 4. Advanced rail defect identification algorithms should also be developed in the future to realize accurate and fast detection of rail damage. It has been investigated that some machine learning algorithms, such as neural network and SVM, show good performance in structural health monitoring. The ultimate goal would be to make automatic identification and classification of rail damage accurately based on the captured signals, which can be achieved by the incorporation of the artificial intelligence algorithms. Rich training data and extraction of effective feature parameters are the crucial areas that need to be focused on in the future.

Declaration of conflicting interests

The author(s) declared no potential conflicts of interest with respect to the research, authorship, and/or publication of this article.

Funding

The author(s) received no financial support for the research, authorship, and/or publication of this article.

ORCID iDs

Hao Ge  <https://orcid.org/0000-0002-8276-2580>
 Yang Yu  <https://orcid.org/0000-0001-9592-8191>

References

1. Ekberg A and Kabo E. Fatigue of railway wheels and rails under rolling contact and thermal loading—an overview. *Wear* 2005; 258: 1288–1300.
2. Clark R. The importance of rail flaw detection to heavy haul operations. In: *Proceedings of the international heavy haul association conference*, Brisbane, QLD, Australia, 10–14 June 2001, vol. 2, pp. 153–161. Virginia, USA: International Heavy Haul Association.
3. Cannon DF, Edel KO, Grassie SL, et al. Rail defects: an overview. *Fatigue Fract Eng Mater Struct* 2003; 26: 865–886.
4. Allison AB. Sperry rail service. *Bull Natl Railway Historical Soc* 1968; 33: 6–10.
5. Federal Railroad Administration (FRA). *Rolling contact fatigue: a comprehensive review*. Washington, DC: FRA, US Department of Transportation, 2011.
6. Grewal DS. Improved ultrasonic testing of railroad rail for transverse discontinuities in the rail head using higher order Rayleigh M21 waves. *Mater Eval* 1996; 54(9): 983–986.
7. Pearson G. Rail testing in the Wessex region. *Insight* 2002; 44(6): 375–378.
8. Rose JL, Avioli MJ, Mudge P, et al. Guided wave inspection potential of defects in rail. *NDT&E Int* 2004; 37(2): 153–161.
9. Lanza di Scalea F, Rizzo P, Coccia S, et al. Non-contact ultrasonic inspection of rails and signal processing for automatic defect detection and classification. *Insight* 2005; 47(6): 346–353.
10. Marais JJ and Mistry KC. Rail integrity management by means of ultrasonic testing. *Fatigue Fract Eng Mater Struct* 2003; 26: 931–938.
11. Clark R and Singh S. The inspection of thermite welds in railroad rail—a perennial problem. *Insight* 2003; 45: 387–393.
12. Hesse D and Cawley P. Surface wave modes in rails. *J Acoust Soc Am* 2006; 120(2): 733–740.
13. Mariani S, Nguyen T, Phillips RR, et al. Noncontact ultrasonic guided wave inspection of rails. *Struct Health Monit* 2013; 12(5–6): 539–548.
14. Wilcox PD, Pavlakovic B, Evans M, et al. Long range inspection of rail using guided waves. *Acta Phys-Chim Sin* 2003; 657(1): 236.
15. Worlton DC. Ultrasonic testing with Lamb waves. *Non-Destruct Test* 1957; 15: 218–222.
16. Rose JL. *Ultrasonic waves in solid media*. New York: Cambridge University Press, 1999.
17. Su Z, Ye L and Lu Y. Guided Lamb waves for identification of damage in composite structures: a review. *J Sound Vib* 2006; 295(3–5): 753–780.
18. Pavlopoulou S, Staszewski WJ and Soutis C. Evaluation of instantaneous characteristics of guided ultrasonic waves for structural quality and health monitoring. *Struct Control Health Monit* 2013; 20(6): 937–955.
19. Aryan P, Kotousov A, Ng CT, et al. A model-based method for damage detection with guided waves. *Struct Control Health Monit* 2017; 24(3): e1884.
20. Nucera C and Lanza di Scalea F. Modeling of nonlinear guided waves and applications to structural health monitoring. *J Comput Civ Eng* 2012; 132(4): 1933.
21. Lowe MJS, Alleyne DN and Cawley P. Defect detection in pipes using guided waves. *Ultrasonics* 1998; 36: 147–154.

22. Alleyne DN, Pavlakovic B, Lowe MJS, et al. Rapid long range inspection of chemical plant pipework using guided waves. *Insight* 2001; 43(2): 93–96.
23. Ghavamian A, Mustapha F and Baharudin BTHT, et al. Detection, localisation and assessment of defects in pipes using guided wave techniques: a review. *Sensors* 2018; 18(12): 4470.
24. Guan R, Lu Y, Wang K, et al. Fatigue crack detection in pipes with multiple mode nonlinear guided waves. *Struct Health Monit* 2019; 18: 180–192.
25. Pavlakovic BN, Lowe MJS and Cawley P. High-frequency low-loss ultrasonic modes in imbedded bars. *Int J Appl Mech* 2001; 68: 67–75.
26. Ghosh T, Kundu T and Karpur P. Efficient use of Lamb modes for detecting defects in large plates. *Ultrasonics* 1998; 36: 791–801.
27. Song WJ, Rose JL, Galan JM, et al. Transmission and reflection of A0 mode Lamb wave in a plate overlap. *AIP Conf Proc* 2003; 657: 1088–1094.
28. Xu K, Ta D, Su Z, et al. Transmission analysis of ultrasonic Lamb mode conversion in a plate with partial-thickness notch. *Ultrasonics* 2014; 54: 395–401.
29. Niu X, Duan W, Chen HP, et al. Excitation and propagation of torsional T(0,1) mode for guided wave testing of pipeline integrity. *Measurement* 2019; 131: 341–348.
30. Li F, Li H, Qiu J, et al. Guided wave propagation in H-beam and probability-based damage localization. *Struct Control Health Monit* 2017; 24(5): e1916.
31. Marzani A. Time-transient response for ultrasonic guided waves propagating in damped cylinders. *Int J Solid Struct* 2008; 45(25–26): 6347–6368.
32. Rose JL, Avioli MJ and Song WJ. Application and potential of guided wave rail inspection. *Insight* 2002; 44(6): 353–358.
33. Hesse D and Cawley P. The potential of ultrasonic surface waves for rail inspection. *AIP Conf Proc* 2004; 24: 227–234.
34. Loveday PW. Guided wave inspection and monitoring of railway track. *J Nondestruct Eval* 2012; 31: 303–309.
35. Wilcox PD, Evans M, Pavlakovic P, et al. Guided wave testing of rail. *Insight* 2003; 45(6): 413–420.
36. Pantano A and Cerniglia D. Simulation of laser generated ultrasound with application to defect detection. *Appl Phys A Mater* 2008; 91: 521–528.
37. Cawley P, Lowe MJS, Alleyne DN, et al. Practical long range guided wave testing: applications to pipes and rail. *Mater Eval* 2003; 61: 66–74.
38. Bartoli I, Lanza di Scalea F, Fateh M, et al. Modeling guided wave propagation with application to the long-range defect detection in railroad tracks. *NDT&E Int* 2005; 38(5): 325–334.
39. Lee C, Rose J and Cho Y. A guided wave approach to defect detection under shelling in rail. *NDT&E Int* 2009; 40(3): 174–180.
40. Ryue J, Thompson D, Whitel P, et al. Investigation of propagating wave types in railway tracks at high frequencies. *J Sound Vib* 2008; 315(1): 157–175.
41. Hayashi T, Song WJ and Rose JL. Guided wave dispersion curves for a bar with an arbitrary cross-section, a rod and rail example. *Ultrasonics* 2003; 41: 175–183.
42. Cannon DF and Pradier H. Rail rolling contact fatigue research by the European Rail Research Institute. *Wear* 1996; 191: 1–13.
43. Care R, Clark S, Dembosky M, et al. Why rails crack: gauge corner cracking on the British network: analysis. *Arup J* 2006; 1: 16–19.
44. Zerbst U, Lundén R, Edel KO, et al. Introduction to the damage tolerance behaviour of railway rails—a review. *Eng Fract Mech* 2009; 76: 2563–2601.
45. Müller S. A linear wheel-rail model to investigate stability and corrugation on straight track. *Wear* 2000; 243: 122–132.
46. Bogdański SB and Brown MW. Modelling the three-dimensional behaviour of shallow rolling contact fatigue cracks in rails. *Wear* 2002; 253(1–2): 17–25.
47. Fisher FD, Daves W, Pippan R, et al. Some comments on surface cracks in rails. *Fatigue Fract Eng Mater Struct* 2006; 29(11): 938–948.
48. Fletcher DI, Smith L and Kapoor A. Rail rolling contact fatigue dependence on friction, predicted using fracture mechanics with a three-dimensional boundary element model. *Eng Fract Mech* 2009; 76(17): 2612–2625.
49. Canadinc D, Sehitoglu H and Verzel K. Analysis of surface crack growth under rolling contact fatigue. *Int J Fatigue* 2008; 30: 1678–1689.
50. Ringsberg JW and Bergkvist A. On propagation of short rolling contact fatigue cracks. *Fatigue Fract Eng Mater Struct* 2003; 26(10): 969–983.
51. Ringsberg JW. Life prediction of rolling contact fatigue crack initiation. *Int J Fatigue* 2001; 23(7): 575–586.
52. Ringsberg JW. Shear mode growth of short surface-breaking RCF cracks. *Wear* 2005; 258(7–8): 955–963.
53. Kondo K, Yoroizaka K and Sato Y. Cause, increase, diagnosis, countermeasures and elimination of Shinkansen shelling. *Wear* 1996; 191: 199–203.
54. Office of Railroad Safety, Federal Railroad Administration. *Track inspector rail defect reference manual*. FRA report, Federal Railroad Administration, Washington, DC, August 2011.
55. Jeong DY and Orringer O. Fatigue crack growth of surface cracks in the rail web. *Theor Appl Fract Mech* 1989; 12: 45–58.
56. Wineman SJ and McClintock FA. Rail web fracture in the presence of residual stresses. *Theor Appl Fract Mech* 1987; 8: 87–99.
57. Clark R. Rail flaw detection: overview and needs for future developments. *NDT&E Int* 2004; 37: 111–118.
58. Li Z, Zhao X, Esveld C, et al. An investigation into the causes of squats—correlation analysis and numerical modeling. *Wear* 2008; 265: 1349–1355.
59. Zumpano G and Meo M. A new damage detection technique based on wave propagation for rails. *Int J Solid Struct* 2006; 43(5): 1023–1046.

60. Murav'ev VV and Boyarkin EV. Nondestructive testing of the structural-mechanical state of currently produced rails on the basis of the ultrasonic wave velocity. *Russ J Nondestr Test* 2003; 39(3): 24–33.
61. Skyttebol A, Josefson BL and Ringsberg JW. Fatigue crack growth in a welded rail under the influence of residual stresses. *Eng Fract Mech* 2005; 72: 271–285.
62. Webster PJ, Wang X, Mills G, et al. Residual stress changes in railway rails. *Phys B Condens Matter* 1992; 180–181: 1029–1031.
63. Zakharov SM and Goryacheva IG. Rolling contact fatigue defects in freight car wheels. *Wear* 2005; 258: 1142–1147.
64. Smith RA. Railway fatigue failures: an overview of a long standing problem. *Materialwiss Werkst* 2005; 36(11): 697–705.
65. Abbaszadeh K, Rahimian M, Toliyat HA, et al. Rail defect diagnosis using wavelet packet decomposition. *IEEE Trans Ind Appl* 2003; 39(5): 1454–1461.
66. Stefano M. *Non-contact ultrasonic guided wave inspection of rails: next generation approach*. ProQuest Dissertations and Theses, University of California, San Diego, CA, 2015.
67. Office of Safety Analysis, Federal Railroad Administration, <http://safetydata.fra.dot.gov/officeofsafety/default.aspx>
68. Rail Accident Investigation Branch. *Class investigation into rail breaks on the East Coast Main Line*. Rail accident report 24/2014, <https://www.gov.uk/raib-reports/test-content/class-investigation-into-rail-breaks-on-the-east-coast-main-line>
69. Pathak M, Alahakoon S, Spiriyagin M, et al. Rail foot flaw detection based on a laser induced ultrasonic guided wave method. *Measurement* 2019; 148: 106922.
70. Wilcox PD, Lowe MJS and Cawley P. The effect of dispersion on long-range inspection using ultrasonic guided waves. *NDT&E Int* 2001; 34(1): 1–9.
71. Wilcox PD. A rapid signal processing technique to remove the effect of dispersion from guided wave signals. *IEEE Trans Ultrason Ferroelectr Freq Control* 2003; 50(4): 419–427.
72. Gazis DC. Three-dimensional investigation of the propagation of waves in hollow circular cylinders. I. analytical foundation. *J Acoust Soc Am* 1959; 31(5): 573–578.
73. Sato K. Elastic wave propagation in an infinite bar of elliptical cross section. *Bull JSME* 1978; 21: 203–209.
74. Mindlin RD and Fox EA. Vibrations and waves in elastic bars of rectangular cross section. *J Appl Mech* 1966; 27: 152–158.
75. Sanderson R and Smith S. The application of finite element modelling to guided ultrasonic waves in rails. *Insight* 2002; 44(6): 359–363.
76. Balasubramanyam R, Quinney D, Challis RE, et al. A finite-difference simulation of ultrasonic Lamb waves in metal sheets with experimental verification. *J Phys D Appl Phys* 1999; 29(1): 147–153.
77. Gavrić L. Computation of propagative waves in free rail using a finite element technique. *J Sound Vib* 1995; 185(3): 531–543.
78. Cho Y and Rose JL. A boundary element solution for a mode conversion study on the edge reflection of Lamb waves. *J Acoust Soc Am* 1996; 99(4): 2097–2109.
79. Cho Y and Rose JL. Boundary element analysis of guided waves in a bar with arbitrary cross-section. *Eng Anal Boundary Elem* 2005; 29: 913–924.
80. Alami B. Waves in prismatic guides of arbitrary cross section. *J Appl Mech* 1973; 40: 1067–1072.
81. Knothe K, Strzyzakowski Z and Willner K. Rail vibrations in the high frequency range. *J Sound Vib* 1994; 169: 111–123.
82. Finnveden S. Spectral finite element analysis of the vibration of straight fluid-filled pipes with flanges. *J Sound Vib* 1997; 199: 125–154.
83. Volovoi VV, Hodges DH, Berdichevsky VL, et al. Dynamic dispersion curves for non-homogeneous, anisotropic beams with cross-section of arbitrary geometry. *J Sound Vib* 1998; 215: 1101–1120.
84. Taweel H, Dong SB and Kazic M. Wave reflection from the free end of a cylinder with an arbitrary cross-section. *Int J Solid Struct* 2000; 37: 1701–1726.
85. Dong SB and Huang KH. Edge vibrations in laminated composite plates. *J Appl Mech* 1985; 52: 433–438.
86. Mukdadi OM and Datta SK. Transient ultrasonic guided waves in layered plates with rectangular cross section. *J Appl Phys* 2003; 93: 9360–9370.
87. Gavrić L. Finite element computation of dispersion properties of thin-walled waveguides. *J Sound Vib* 1994; 173: 113–124.
88. Wilcox PD, Evans M, Diligent O, et al. Dispersion and excitability of guided acoustic waves in isotropic beams with arbitrary cross section. *AIP Conf Proc* 2002; 21: 203–210.
89. Hayashi T, Kawashima K and Rose JL. Calculation for guided waves in pipes and rails. *Key Eng Mater* 2004; 270: 410–415.
90. Coccia S, Bartoli I, Marzani A, et al. Numerical and experimental study of guided waves for detection of defects in the rail head. *NDT&E Int* 2011; 44(1): 93–100.
91. Bartoli I, Marzani A, Lanza di Scalea F, et al. Modeling wave propagation in damped waveguides of arbitrary cross-section. *J Sound Vib* 2006; 295: 685–707.
92. Nilsson CM, Jones CJC, Thompson DJ, et al. A wave-guide finite element and boundary element approach to calculating the sound radiated by railway and tram rails. *J Sound Vib* 2009; 321(3–5): 813–836.
93. Ryue J, Thompson DJ, White PR, et al. Decay rates of propagating waves in railway tracks at high frequencies. *J Sound Vib* 2009; 320(4–5): 955–976.
94. Ryue J, Thompson DJ, White PR, et al. Investigations of propagating wave types in railway tracks at high frequencies. *J Sound Vib* 2008; 315(1–2): 157–175.
95. Li W, Dwight RA and Zhang T. On the study of vibration of a supported railway rail using the semi-analytical finite element method. *J Sound Vib* 2015; 345: 121–145.
96. Knothe K and Grassie SL. Modelling of railway track and vehicle/track interaction at high frequencies. *Vehicle Syst Dyn* 1993; 22: 209–262.

97. Damljanović V and Weaver RL. Laser vibrometry technique for measurement of contained stress in railroad rail. *J Sound Vib* 2005; 282(1–2): 341–366.
98. Chen F and Wilcox PD. The effect of load on guided wave propagation. *Ultrasonics* 2008; 47(1–4): 111–122.
99. Loveday PW. Semi-analytical finite element analysis of elastic waveguides subjected to axial loads. *Ultrasonics* 2009; 49: 298–300.
100. Michael L and Brian P. *Disperse-a system for generating dispersion curves-user's manual*. UK: Imperial College Consultants, 2013
101. Hayashi T, Miyazaki Y, Murase M, et al. Guided wave inspection for bottom edge of rails. *AIP Conf Proc* 2007; 894: 169.
102. Hayashi T, Kataoka K, Takikawa M. Modal analysis of guided waves and its application to rail inspection. *J Solid Mech Mater Eng* 2008; 2(10): 1298–1306.
103. Bocchini P, Marzani A and Viola E. Graphical user interface for guided acoustic waves. *J Comput Civ Eng* 2011; 25: 202–210.
104. Calle Herrero FJ, Garcia DF and Usamentiaga R. Inspection system for rail surfaces using differential images. *IEEE Trans Ind Appl* 2018; 54: 4948–4957.
105. Wang L, Zhuang L and Zhang Z. Automatic detection of rail surface cracks with a superpixel-based data-driven framework. *J Comput Civ Eng* 2019; 33: 4018053.
106. Li Q and Ren S. A real-time visual inspection system for discrete surface defects of rail heads. *IEEE T Instrum Meas* 2012; 61(8): 2189–2199.
107. Mazzeo PL, Nitti M, Stella E, et al. Visual recognition of fastening bolts for railroad maintenance. *Pattern Recogn Lett* 2004; 25(6): 669–677.
108. Allan MZ, Todd LE and Joseph WP. Development, implementation, and validation of an automated turnout inspection vehicle, <http://www.railway-technology.com/downloads/whitepapers/track/file2286>
109. ENSCO. Track imaging systems-machine vision high-resolution rail inspection-track defects, <http://ensco.com/rail/track-imaging-systems>
110. Marino F, Distante A, Mazzeo P, et al. A real-time visual inspection system for railway maintenance: automatic hexagonal-headed bolts detection. *IEEE Trans Syst Man Cyb C* 2007; 3(37): 418–428.
111. Cantero D and Basu B. Railway infrastructure damage detection using wavelet transformed acceleration response of traversing vehicle. *Struct Control Health Monit* 2014; 22: 62–70.
112. Remennikov AM and Kaewunruen S. A review of loading conditions for railway track structures due to train and track vertical interaction. *Struct Control Health Monit* 2008; 15(2): 207–234.
113. Molodova M, Oregui M, Núñez A, et al. Health condition monitoring of insulated joints based on axle box acceleration measurements. *Eng Struct* 2016; 123(15): 225–235.
114. Li Z, Molodova M, Núñez A, et al. Improvements in axle box acceleration measurements for the detection of light squats in railway infrastructure. *IEEE T Ind Electron* 2015; 62(7): 4385–4397.
115. Wei Z, Alfredo N, Li Z, et al. Evaluating degradation at railway crossings using axle box acceleration measurements. *Sensors* 2017; 17(10): 2236.
116. Oregui M, Li S, Núñez A, et al. Monitoring bolt tightness of rail joints using axle box acceleration measurements. *Struct Control Health Monit* 2017; 24(2): 1848.
117. Ph Papaelias M, Roberts C and Davis CL. A review on non-destructive evaluation of rails: state-of-the-art and future development. *Proc IMechE, Part F: Journal of Rail and Rapid Transit* 2008; 222(4): 367–384.
118. Javier GM, Jaime GG and Ernesto VS. Non-destructive techniques based on eddy current testing. *Sensors* 2011; 11(3): 2525–2565.
119. Rajamaki J, Vippola M, Nurmioku A, et al. Limitations of eddy current inspection in railway rail evaluation. *Proc IMechE, Part F: Journal of Rail and Rapid Transit* 2018; 232: 121–129.
120. Pohl R, Krull R and Meierhofer R. A new eddy current instrument in a grinding train. In: *Proceedings of the ECNDT 2006*, Berlin, 25–29 September 2006.
121. Thomas HM, Junger M, Hintze H, et al. Pioneering inspection of railroad rails with eddy currents. In: *Proceedings of the 15th world conference on non-destructive testing*, Rome, 15–21 October 2000.
122. Pohl R, Erhard A, Montag HJ, et al. NDT techniques for railroad wheel and gauge corner inspection. *NDT&E Int* 2004; 37(2): 89–94.
123. Junger M, Thomas HM, Krull R, et al. The potential of eddy current technology regarding railroad inspection and its implementation. In: *Proceedings of the 16th world conference on non-destructive testing*, Montreal, QC, Canada, 30 August–3 September 2004.
124. Thomas HM, Heckel T and Hanspach G. Advantage of a combined ultrasonic and eddy current examination for railway inspection trains. In: *Proceedings of the ECNDT 2006*, Berlin, 25–29 September 2006.
125. Bray DE and Stanley RK. *Non-destructive evaluation: a tool in design, manufacturing, and service*. West Palm Beach, FL: CRC Press, 1997, pp. 215–427.
126. Kenzo M. Recent advancement of electromagnetic non-destructive inspection technology in Japan. *IEEE Trans Magnet* 2002; 38(2): 321–326.
127. Drury JC and Pearson N. Corrosion detection in ferrite steels using magnetic flux leakage. In: *Proceedings of the magnetism in non-destructive testing*, London, 12 April 2005.
128. Clark R, Main JD and Boyle J. *A new approach to the use of induction for rail inspection*. London: Railway Engineering, 2000.
129. Papaelias MP, Lugg MC, Roberts C, et al. High-speed inspection of rails using ACFM techniques. *NDT&E Int* 2009; 42(4): 328–335.
130. Nicholson GL, Kostryzhev AG, Hao XJ, et al. Modelling and experimental measurements of idealised and light-moderate RCF cracks in rails using an ACFM sensor. *NDT&E Int* 2011; 44(5): 427–437.

131. Papaelias MP, Roberts C, Davis CL, et al. Detection and quantification of rail contact fatigue cracks in rails using ACFM technology. *Insight* 2008; 50(7): 364–368.
132. Rowshandel H, Papaelias M, Roberts C, et al. Development of autonomous ACFM rail inspection techniques. *Insight* 2011; 53(2): 85–89.
133. Rowshandel H, Nicholson GL, Davis CL, et al. A robotic approach for NDT of RCF cracks in rails using an ACFM sensor. *Insight* 2011; 53(7): 368–376.
134. Low CK and Wong BS. Defect evaluation using the alternating current field measurement technique. *Insight* 2004; 46(10): 598–605.
135. Howitt M. Bombardier brings ACFM into the rail industry. *Insight* 2002; 44(6): 379–382.
136. Yu J, Ziehl P, Boris Z, et al. Prediction of fatigue crack growth in steel bridge components using acoustic emission. *J Constr Steel Res* 2011; 67(8): 1254–1260.
137. Tsangouri E and Aggelis DG. A review of acoustic emission as indicator of reinforcement effectiveness in concrete and cementitious composites. *Constr Build Mater* 2019; 224: 198–205.
138. Bruzelius K and MBA D. An initial investigation on the potential applicability of acoustic emission to rail track fault detection. *NDT&E Int* 2004; 37(7): 507–516.
139. Wang J, Liu XZ and Ni YQ. A Bayesian probabilistic approach for acoustic emission-based rail condition assessment. *Comput-Aided Civ Infrastruct Eng* 2018; 33(1): 21–34.
140. Hao Q, Zhang X, Wang Y, et al. A novel rail defect detection method based on undecimated lifting wavelet packet transform and Shannon entropy-improved adaptive line enhancer. *J Sound Vib* 2018; 425: 208–220.
141. Zhang X, Zou Z, Wang K, et al. A new rail crack detection method using LSTM network for actual application based on AE technology. *Appl Acoust* 2018; 142(12): 78–86.
142. Xin Z, Qiushi H, Kangwei W, et al. An investigation on acoustic emission detection of rail crack in actual application by chaos theory with improved feature detection method. *J Sound Vib* 2018; 436: 165–182.
143. Zhang J, Ma H, Yan W, et al. Defect detection and location in switch rails by acoustic emission and Lamb wave analysis: a feasibility study. *Appl Acoust* 2016; 105(4): 67–74.
144. Li D, Kuang KSC and Koh CG. Rail crack monitoring based on Tsallis synchrosqueezed wavelet entropy of acoustic emission signals: a field study. *Struct Health Monit* 2017; 17(6): 1410–1424.
145. Li D, Kuang KSC and Koh CG. Fatigue crack sizing in rail steel using crack closure-induced acoustic emission waves. *Meas Sci Technol* 2017; 28(6): 065601.
146. Thompson DJ. Experimental analysis of wave propagation in railway tracks. *J Sound Vib* 1997; 203: 867–888.
147. Guillermo MV, Alan CDV, Ezequiel AGH, et al. Experimental and numerical study for detection of rail defect. *Eng Fail Anal* 2017; 81: 94–102.
148. Loveday PW. Development of piezoelectric transducers for a railway integrity monitoring system. *Proc SPIE* 2000; 3988: 330–338.
149. Burger FA. A practical continuous operating rail break detection system using guided waves. In: *Proceedings of the 18th world conference on non-destructive testing*, Durban, South Africa, 16–20 April 2012.
150. Gharaibeh Y, Sanderson R, Mudge P, et al. Investigation of the behaviour of selected ultrasonic guided wave modes to inspect rails for long-range testing and monitoring. *Proc IMechE, Part F: Journal of Rail and Rapid Transit* 2011; 225: 311–324.
151. Moustakidis S, Kappatos V, Karlsson P, et al. An intelligent methodology for railways monitoring using ultrasonic guided waves. *J Nondestruct Eval* 2014; 33: 694–710.
152. Wilkinson A. Long range inspection and condition monitoring of rails using guided waves. In: *Proceedings of the 51st annual conference of the British institute of nondestructive testing*, Daventry, 11–13 September 2012, pp. 165–175, https://www.bindt.org/downloads/NDT 2012_2C5.pdf
153. Moustakidis S, Kappatos V, Karlsson P, et al. An automated long range ultrasonic rail flaw detection system based on the support vector machine algorithm. In: *Proceedings of the computers in railways XIII: computer system design and operation in the railway and other transit systems*, New Forest, 11–13 September 2012, vol. 127, pp. 199–210. Southampton: WIT Press.
154. Cawley P, Lowe MJS, Alleyne DN, et al. Practical long range guided wave inspection-applications to pipes and rail. *Mater Eval* 2003; 61: 66–74.
155. Cawley P, Wilcox PD, Alleyne DN, et al. Long range inspection of rail using guided waves—field experience. In: *Proceedings of the 16th world conference on non-destructive testing*, Montreal, QC, Canada, 30 August–3 September 2004.
156. Hayashi T. Guided wave dispersion curves derived with a semianalytical finite element method and its applications to nondestructive inspection. *Jpn J Appl Phys* 2008; 47: 3865–3870.
157. Zhou C, Zhang C, Su Z, et al. Health monitoring of rail structures using guided waves and three-dimensional diagnostic imaging. *Struct Control Health Monit* 2017; 24(9): e1966.
158. Dutton B, Clough AR, Rosli MH, et al. Non-contact ultrasonic detection of angled surface defects. *NDT&E Int* 2011; 44(4): 353–360.
159. Dixon S, Burrows SE, Dutton B, et al. Detection of cracks in metal sheets using pulsed laser generated ultrasound and EMAT detection. *Ultrasonics* 2011; 51(1): 7–16.
160. Cerniglia D, Pantano A and Vento MA. Guided wave propagation in a plate edge and application to NDI of rail base. *J Nondestruct Eval* 2012; 31(3): 245–252.
161. Kenderian S, Cerniglia D, Djordjevic B, et al. Rail track field testing using laser/air hybrid ultrasonic technique. *Mater Eval* 2003; 61: 1129–1133.
162. Cerniglia D, Garcia G, Kalay S, et al. Application of laser induced ultrasound for rail inspection. In: *Proceedings of the 7th world congress on railway research (WCRR)*, Montreal, QC, Canada, 4–8 June 2006, pp. 1–7, <http://www.railway-research.org/IMG/pdf/272-2.pdf>

163. Kenderian S, Djordjevic B and Green RE. Laser based and air coupled ultrasound as non-contact and remote techniques for testing of railroad tracks. *Mater Eval* 2002; 60: 65–70.
164. Kenderian S, Djordjevic BB, Cerniglia D, et al. Dynamic railroad inspection using the laser-air hybrid ultrasonic technique. *Insight* 2006; 48: 336–341.
165. Nielsen SA and Hesthaven JS. A multi-domain Chebychev collocation method for predicting ultrasonic field parameters in complex material geometries. *Ultrasonics* 2002; 40(1–8): 177–180.
166. Nielsen SA, Bardenshtein AL, Thommesen AM, et al. Non-contact ultrasound for industrial process monitoring of moving objects. *Rev Prog QNDE* 2004; 23: 1499–1506.
167. Nielsen SA, Bardenshtein AL, Thommesen AM, et al. Automatic laser ultrasonics for rail inspection. In: *Proceedings of the 16th world conference on non-destructive testing*, Montreal, QC, Canada, 30 August–3 September 2004, p. 30, https://www.ndt.net/article/wcndt2004/pdf/laser_ultrasonics/377_nielsen.pdf
168. Coccia S. *Ultrasonic guided waves for structural health monitoring and application to rail inspection prototype for the Federal Railroad Administration*, UC San Diego Electronic Theses and Dissertations, ProQuest Dissertations Publishing, Ann Arbor, MI, 2007.
169. Coccia S, Phillips R, Bartoli I, et al. Noncontact ultrasonic guided-wave system for rail inspection: update on project at University Of California, San Diego. *Transp Res Rec* 2011; 2261: 143–147.
170. Mcnamara J and Lanza di Scalea F. Improvements in non-contact ultrasonic testing of rails by the discrete wavelet transform. *Mater Eval* 2004; 62(3): 365–372.
171. Rizzo P and Lanza di Scalea F. Discrete wavelet transform to improve guided-wave-based health monitoring of tendons and cables. *Proc SPIE* 2004; 5391: 523–532.
172. Mariani S and Lanza di Scalea F. Predictions of defect detection performance of air-coupled ultrasonic rail inspection system. *Struct Health Monit* 2018; 17: 684–705.
173. Mariani S, Nguyen T, Zhu X, et al. Field test performance of noncontact ultrasonic rail inspection system. *J Transp Eng A Syst* 2017; 143(5): 04017007.
174. Mariani S, Nguyen TV, Zhu X, et al. Non-contact ultrasonic guided wave inspection of rails: field test results and updates. *Proc SPIE* 2017; 9435: 94351O.
175. Ryue J, Thompson DJ, White PR, et al. Wave reflection and transmission due to defects in infinite structural waveguides at high frequencies. *J Sound Vib* 2011; 330(8): 1737–1753.
176. Lanza di Scalea F, Sternini S and Liang AY. Robust passive reconstruction of dynamic transfer function in dual-output systems. *J Acoust Soc Am* 2018; 143: 1019–1028.
177. Lanza di Scalea F, Zhu X, Capriotti M, et al. High-speed non-contact ultrasound system for rail track integrity evaluation. In: *Proceedings of the health monitoring of structural and biological systems XII*, Denver, CO, 27 March 2018.
178. Lanza di Scalea F, Zhu X, Capriotti M, et al. Passive extraction of dynamic transfer function from arbitrary ambient excitations: application to high-speed rail inspection from wheel-generated waves. *J Nondestruct Eval* 2018; 1: 011005.
179. Wang K, Cao W, Xu L, et al. Diffuse ultrasonic wave-based structural health monitoring for railway turnouts. *Ultrasonics* 2020; 101: 106031.
180. Hirao M and Ogi H. *EMATs for science and industry: noncontacting ultrasonic measurements*. Boston, MA: Springer, 2003.
181. Chahbaz A. Development of a mobile inspection system for rail integrity assessment. *J Soc Nav Archit Jpn* 2000; 188: 351–358.
182. Chahbaz A, Brassard M and Pelletier A. Mobile inspection system for rail integrity assessment. In: *Proceedings of the 15th world conference of non-destructive testing*, Rome, 15–21 October 2000.
183. Dixon S, Edwards RS and Jian X. Inspection of the rail-track head surfaces using electromagnetic acoustic transducers. *Insight* 2004; 46: 326–330.
184. Edwards RS, Dixon S and Jian X. Characterisation of defects in the railhead using ultrasonic surface waves. *NDT&E Int* 2006; 39: 468–475.
185. Edwards RS, Dixon S and Jian X. Depth gauging of defects using low frequency wideband Rayleigh waves. *Ultrasonics* 2006; 44: 93–98.
186. Fan Y, Dixon S, Edwards RS, et al. Ultrasonic surface wave propagation and interaction with surface defects on rail track head. *NDT&E Int* 2007; 40: 471–477.
187. Wang S, Chen X, Jiang T, et al. Electromagnetic ultrasonic guided waves inspection of rail base. In: *Proceedings of the IEEE Far East forum on nondestructive evaluation/testing*, Chengdu, China, 20–23 June 2014, pp. 135–139. New York: IEEE.